



Contents lists available at ScienceDirect

Earth and Planetary Science Letters

journal homepage: www.elsevier.com/locate/epsl

Cosmogenic ^{26}Al in the atmosphere and the prospect of a $^{26}\text{Al}/^{10}\text{Be}$ chronometer to date old ice

Matthias Auer ^{a,*}, Dietmar Wagenbach ^b, Eva Maria Wild ^a, Anton Wallner ^a, Alfred Priller ^a, Heinrich Miller ^c, Clemens Schlosser ^d, Walter Kutschera ^a

^a VERA Laboratory, Fakultät für Physik, Universität Wien, Währingerstr. 17, 1090, Wien, Austria

^b Institut für Umweltphysik, Rupprecht-Karls-Universität Heidelberg, Im Neuenheimer, Feld 229, D-69120 Heidelberg, Germany

^c Alfred-Wegener-Institut für Polar- und Meeresforschung, Columbusstrasse, D-27568 Bremerhaven, Germany

^d Bundesamt für Strahlenschutz, Rosastr. 9, D-79098 Freiburg, Germany

ARTICLE INFO

Article history:

Received 8 May 2009

Received in revised form 19 August 2009

Accepted 25 August 2009

Available online xxxx

Editor: P. DeMenocal

Keywords:

^{26}Al

^{10}Be

accelerator mass spectrometry

dating

cosmogenic radionuclides

ABSTRACT

Cosmogenic radionuclides in the one-million-year half-life range offer unique possibilities for age determinations in geophysics. In measurements where the radioactive decay is being utilized as a clock, uncertainties in age determinations may be reduced if the ratio of two radioisotopes with different half-lives can be used as a chronometer. In this work we investigate the atomic ratio of atmospheric ^{26}Al ($t_{1/2} = 0.717$ Ma) to ^{10}Be ($t_{1/2} = 1.387$ Ma) measured with accelerator mass spectrometry (AMS), and its potential as a chronometer for dating old ice. The $^{26}\text{Al}/^{10}\text{Be}$ ratio decreases with an effective half-life of $t_{1/2}(^{26}\text{Al}/^{10}\text{Be}) = 1.48$ Ma. For its application as a chronometer, the atmospheric $^{26}\text{Al}/^{10}\text{Be}$ ratio has to be well characterized. However, the properties of atmospheric ^{26}Al have been understood only poorly so far. At the VERA AMS facility of the University of Vienna, a first systematic study of the global variations of the $^{26}\text{Al}/^{10}\text{Be}$ ratio in the atmosphere and in surface firn has been carried out, and pilot measurements of the $^{26}\text{Al}/^{10}\text{Be}$ ratio in deep Antarctic ice have been performed. Our results indicate that this ratio is globally constant to within 5% in the atmosphere and in surface firn with a mean value of 1.89×10^{-3} . The data also suggest that non-atmospheric sources of ^{26}Al , such as extraterrestrial, in situ produced or re-suspended ^{26}Al , do not contribute significantly to the observed $^{26}\text{Al}/^{10}\text{Be}$ ratio. In addition, atmospheric mixing seems to exert only a minor influence. In a first application of the method, $^{26}\text{Al}/^{10}\text{Be}$ ratios were measured in chips collected in connection with the drilling of the lowest part of an ice core (2250 to 2760 m) in Dronning Maud Land, Antarctica. Surprisingly, variable $^{26}\text{Al}/^{10}\text{Be}$ ratios ranging between 0.5 and up to 2 times the atmospheric ratio were found at different locations in this deep ice core. While the cause for the ratios higher than atmospheric remains unexplained so far, the ratios lower than atmospheric may be caused by radioactive decay, allowing a first dating attempt using the $^{26}\text{Al}/^{10}\text{Be}$ ratio. Thus, at an ice depth of 2760 m an approximate date of $(6.7 \pm 2.6) \times 10^5$ years was established.

© 2009 Elsevier B.V. All rights reserved.

1. Introduction

The cosmogenic radionuclide ^{26}Al has been used primarily for the investigation of the history and exposure ages of terrestrial rocks (Nishiizumi et al., 1991; Strack et al., 1994; Burbank et al., 1996; Pavicevic et al., 2004), and of meteorites (Nishiizumi et al., 1986), where ^{26}Al is among the most abundant long-lived cosmogenic radionuclides. The half-life of ^{26}Al is $t_{1/2} = (7.17 \pm 0.24) \times 10^5$ a, calculated as the weighted mean with standard deviation of the values reported in Samworth et al. (1972), Middleton et al. (1983), Norris et al. (1983), and Thomas et al. (1984). ^{26}Al is also produced in the atmosphere by spallation of argon by highly energetic cosmic rays (hereinafter referred to as meteoric ^{26}Al), however with a relatively low global production rate reported between

1.6×10^3 ^{26}Al atoms $\text{cm}^{-2} \text{a}^{-1}$ (J. Beer, pers. comm.) and 4.4×10^3 ^{26}Al atoms $\text{cm}^{-2} \text{a}^{-1}$ (Lal and Peters, 1967). Tropospheric concentrations are in the order of 100 atoms/ m^3 only, about 500 times lower than e.g. those of the cosmogenic radionuclide ^{10}Be . The half-life of ^{10}Be has been under debate for some time (Fink and Smith, 2007; Nishiizumi et al., 2007), and has recently been re-determined with high precision (Korschinek, submitted for publication). From these new measurements one obtains a value of $t_{1/2} = (1.387 \pm 0.012) \times 10^6$ a for the half-life of ^{10}Be .

Like ^{10}Be , ^{26}Al becomes quickly attached to aerosol particles, with which it shares its atmospheric cycle including wet and dry deposition. Due to its low concentrations, studies of meteoric ^{26}Al and its preservation in sedimentary archives are scarce. First measurements of ^{26}Al concentrations in the atmosphere by accelerator mass spectrometry (AMS) were performed already some 20 years ago (Raisbeck et al., 1983; Middleton and Klein, 1987). Further, ^{26}Al was measured in ocean sediments. However, since AMS measurement of $^{26}\text{Al}/^{27}\text{Al}$ in sediments is complicated by high ^{27}Al concentrations, only a few

* Corresponding author. Now at Bundesamt für Strahlenschutz, Rosastr. 9, D-79098 Freiburg, Germany. Tel.: +49 30 18 333 6776; fax: +49 30 18 10333 6776.

E-mail address: m.auer1@gmx.de (M. Auer).

studies of ^{26}Al in sediments have been published (Wang et al., 1996; Luo et al., 2001). Only recently new data on atmospheric ^{26}Al concentrations have become available (Auer et al., 2007; Horiuchi et al., 2007), but no systematic investigation of its sources, properties and potential applications has been performed so far. Aimed at exploring applications of ^{26}Al in atmospheric and climate research, the present study attempts to experimentally investigate the various sources and deposition properties of ^{26}Al in the atmosphere.

A potential application of meteoric ^{26}Al is dating of very old ice archives, by measurements in combination with ^{10}Be . Since in situ production may be neglected (Lal et al., 1987), the glacial $^{26}\text{Al}/^{10}\text{Be}$ ratio in polar ice sheets is only determined by the initial value in surface firn and by radioactive decay. Note that the ^{10}Be and ^{26}Al concentrations in the atmosphere strongly depend on meteorological conditions and on production rate variability. Since these interferences are expected to affect both nuclides in a similar way, the $^{26}\text{Al}/^{10}\text{Be}$ ratio should be only governed by radioactive decay. The $^{26}\text{Al}/^{10}\text{Be}$ atomic ratio decreases with an effective half-life of $t_{1/2} (^{26}\text{Al}/^{10}\text{Be}) = (1.48 \pm 0.04) \times 10^6$ a, allowing for calculating the sample age t according to:

$$t = (t_{1/2} / \ln 2) \times \ln(R_0 / R_t)$$

where R_0 and R_t are the ratios of $^{26}\text{Al}/^{10}\text{Be}$ in the atmosphere and at time t , respectively. The accuracy of this method is largely limited by the precision of the AMS measurement of the $^{26}\text{Al}/^{10}\text{Be}$ ratio, which is currently 10% at best for typical samples (Auer et al., 2007) and which is dominated by the ^{26}Al counting statistics. This translates to a minimum age uncertainty of 2.2×10^5 years, which makes this dating method applicable for ice which is older than several 10^5 years.

Alternatively to ^{26}Al , meteoric ^{36}Cl might be used together with ^{10}Be , which has a shorter half-life of $t_{1/2} = (3.01 \pm 0.02) \times 10^5$ a (Endt, 1990). However, since atmospheric Cl species also form gaseous HCl, the $^{36}\text{Cl}/^{10}\text{Be}$ ratio may be altered significantly already in the atmosphere and particularly after deposition onto the snow surfaces. The latter effect is very substantial at low accumulation sites in Antarctica (Röthlisberger et al., 2003; Delmas et al., 2004; Weller et al., 2004). However, $^{36}\text{Cl}/^{10}\text{Be}$ dating has been recently applied to deep ice cores from Greenland (Willerslev et al., 2007).

Before applying the $^{26}\text{Al}/^{10}\text{Be}$ dating method for ice samples, one has to verify that the atmospheric $^{26}\text{Al}/^{10}\text{Be}$ ratio is sufficiently constant and that its initial firm value is not significantly altered by post depositional processes. In the following, potential factors which may cause variations of this ratio are discussed. The atmospheric production of ^{26}Al and ^{10}Be is a function of the energy dependent cross sections. While ^{10}Be production is maximal for neutron energies around 20 MeV (Nakamura et al., 1992), production of ^{26}Al becomes effective for neutron and proton energies above 100 MeV (Kubo, 2001). Since the relative contribution of low energetic neutrons to the cosmic radiation increases with atmospheric depth (Lal and Peters, 1967), differences of 30 to 50% between the stratospheric and tropospheric $^{26}\text{Al}/^{10}\text{Be}$ production ratio may, be possible, while the dependence on temporal variations of the geomagnetic field strength and of the solar wind is much weaker (Masarik and Beer, 1999; Beer, pers. comm.).

Variation of atmospheric production is not the only mechanism which might influence the atmospheric $^{26}\text{Al}/^{10}\text{Be}$ ratio. ^{26}Al produced in meteorites and interplanetary dust (denoted as extraterrestrial ^{26}Al) and in terrestrial rock mobilized as mineral dust (denoted as in situ produced ^{26}Al) may add to the atmospheric ^{26}Al budget. For ^{10}Be these sources are negligible, because of its 500 fold higher atmospheric production rate. The strength of the extraterrestrial ^{26}Al source depends on the rate of accretion of extraterrestrial material, but also on its exposure history and composition. Lal and Jull (2003) estimate an accretion of 74 atoms/cm² a of ^{26}Al produced in meteorites, corresponding roughly to 6% of the atmospheric production, which provides a lower limit since they neglect the possibly significant contribution of ^{26}Al produced by solar cosmic rays in interplanetary dust (Tanaka et al., 1972; Michel et al., 1982; Nishiizumi

et al., 1995). Since a fraction of up to 90% of the accreted extraterrestrial material evaporates during entry into the atmosphere (Love and Brownlee, 1991), most extraterrestrial ^{26}Al may be incorporated in small particles and likely get mixed with meteoric ^{26}Al . Nothing is known yet about the in situ produced ^{26}Al flux to the atmosphere, or about the remobilization of meteoric ^{26}Al and ^{10}Be entering the atmosphere as re-suspended nuclides carried by mobilized mineral dust.

Data on atmospheric ^{26}Al have been too sparse to allow for verification of the production rate calculations and to estimate the possible effect of extraterrestrial or terrestrial ^{26}Al contributions. Also post-deposition effects on the $^{26}\text{Al}/^{10}\text{Be}$ ratio in the glacier archive have so far not been investigated. In order to test the potential of using $^{26}\text{Al}/^{10}\text{Be}$ to date old ice bodies, we tackled these issues in three steps. First, the geographic and temporal variability of atmospheric ^{26}Al and ^{10}Be was investigated and compared with that expected from calculated atmospheric production rates of ^{26}Al and ^{10}Be in high geographical resolution, using the model from Masarik and Beer (1999). In a next step the air to firm transfer of ^{26}Al and ^{10}Be was studied by measurement of surface firn samples from Antarctica. Finally, first analyses of ^{26}Al and ^{10}Be in the bottom part of a deep Antarctic ice core were made.

2. Methods

2.1. Experimental approach

In order to characterize the atmospheric variability of the $^{26}\text{Al}/^{10}\text{Be}$ ratio we selected tropospheric aerosol samples (covering seasonal to multi-year time scales) from different geographic regions, distinguished by different mineral dust contributions. In order to infer the possible influence of the vertical change in the $^{26}\text{Al}/^{10}\text{Be}$ production ratio, we also investigated stratospheric aerosol samples. So far, these analyses do not necessarily provide information on the extraterrestrial ^{26}Al input, which is expected to be rather homogeneously distributed in the atmosphere and may not cause distinct geographical or short term changes of the atmospheric $^{26}\text{Al}/^{10}\text{Be}$ ratio. For this purpose we have measured ^{53}Mn ($t_{1/2} = (3.7 \pm 0.4) \times 10^6$ a (Honda and Imamura, 1971)), a proxy for meteoritic matter, in a few selected aerosol samples and in one surface ice sample. ^{53}Mn is produced by cosmic rays interactions on iron in meteoroids (Leya et al., 2000) and interplanetary dust (Reedy, 1990), but due to lack of target atoms there is almost no production in the atmosphere. Analytical details of our ^{53}Mn measurements will be presented in a forthcoming publication.

For investigating the effect of air/firn transfer on the $^{26}\text{Al}/^{10}\text{Be}$ ratio, we have focused on Antarctic firn samples, taken from coastal high accumulation areas, where atmospheric observation also have been obtained, and from low accumulation deep drilling sites on the Antarctic plateau. Thus ^{26}Al and ^{10}Be samples covering a large range of glacio-meteorological conditions were obtained, partly allowing also for direct comparison with the respective atmospheric values.

2.2. Sample selection

An overview on aerosol, firn and ice samples measured in this study is given in Table 1. The European aerosol sampling sites at Schauinsland and Sonnblick are characterized by relatively high concentrations of terrestrial dust (on the order of 100 to 1000 ng/m³, derived from the concentrations of aluminum in the samples), while the Antarctic site at Neumayer has very low dust levels in the order of 10 ng/m³ (Wagenbach, 1994), allowing for the investigation of the influence of terrestrial and re-suspended ^{26}Al and ^{10}Be . A subset of these measurements has already been previously published (Auer et al., 2007). We have also extended our study to stratospheric aerosol samples, which were taken in Sweden on a 1 hour flight on 12 December 2004 at an altitude of 12.5 km.

Fig. 1 shows the sampling sites of our Antarctic firn and ice samples. The surface samples from Neumayer correspond closely to the position of the aerosol sampling station. Deep ice core samples were selected from 2554 to 2760 m depth of the EPICA-EDML core

Table 1
Overview and characterization of ^{26}Al and ^{10}Be samples.

Aerosol samples				
Sampling location (Lat., Long.)	Sample volume (m ³)	Number of samples (sampling time)	Classification	
Sonnblick (47°03' N, 12°58' E)	~10000	20 (1 d)	Mid latitude, high alpine (3106 m a.s.l.), episodically strong terrestrial dust input	
Schauinsland (47°54' N, 7°54' E)	~10000	6 (7 d)	Mid latitude, (1200 m a.s.l.), medium terrestrial dust level	
Sweden	100	6(½ h)	Mid latitude high altitude (12500 m a.s.l.), lower stratosphere/upper troposphere, extremely low terrestrial dust	
Neumayer single (70°39' S, 08°15' W)	~10000	6 (~10 d)	High latitude, sea level, extremely low terrestrial dust	
Neumayer composite	~50000	9 (½ a)	High latitude, sea level, extremely low terrestrial dust	
Antarctic firn and ice samples				
Sampling location (Lat., Long.)	Sample mass	Mean accumulation rate (g/cm ² a)	Number of samples (time coverage)	Classification
Neumayer (70°39' S, 08°15' W)	4–6.5 kg	36 ^a	4 (several months)	Surface snow, high accumulation
Kohnen (75°00' S, 00°04' E)	180 kg	6.4 ^b	1 (2 a)	Surface firn, altitude (2892 a.s.l.), low accumulation
Kohnen	4 to 16 kg	~3–~10 ^c	12 (several ka)	Drill chips from the EPICA-EDML deep ice core, depth 2554 to 2760 m
Dome C (75° 06' S, 123° 24')	3–6 kg	2.5 ^d	7 (up to 100 a)	Surface firn and firn core from 0 to 12 m depth, (3233 m a.s.l.), extremely low accumulation
Cap Prudomme	4–6 kg	Unknown	4 (unknown)	Ice samples from glacier terminus

^a Schlosser et al. (2002).

^b (Epica, 2006).

^c (Range for the whole ice core (EPICA, 2006)).

^d (Epica, 2004).

drilled at Kohnen Station. They are thus outside the dated section of the core, which extends to a depth of 2400 m, corresponding to 150 000 years (Ruth et al., 2007). The deepest samples are taken close to the bedrock at (2782 ± 10) m depth (F. Wilhelms, pers. comm.) for which a first application of the $^{26}\text{Al}/^{10}\text{Be}$ dating method was envisaged. Since several kg of ice are required for sufficiently precise ^{26}Al measurements, the actual ice core could not be used for this pilot study. Therefore, drill chips of the EDML core were used instead, which were sampled at approximately one meter depth resolution and which provide typically several kg of ice per sample.

2.3. Sample preparation

The purpose of the sample preparation procedure is to extract Al and Be from the aerosol filter and melt water samples and convert

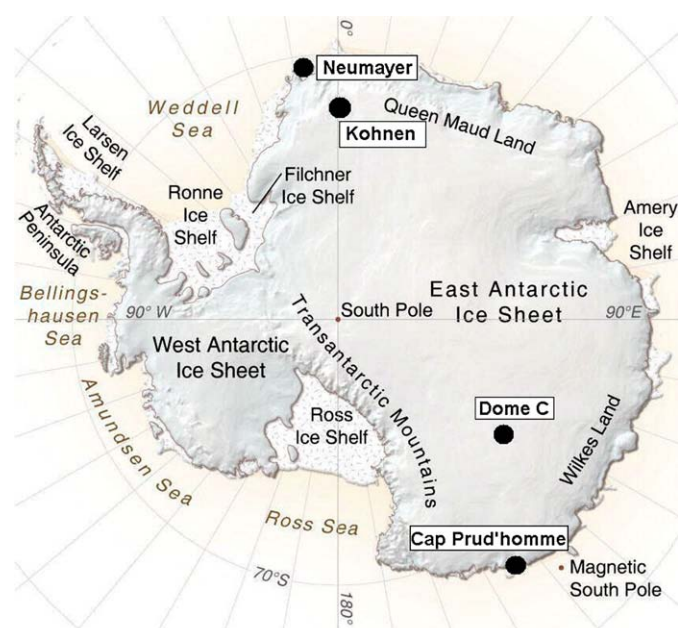


Fig. 1. Antarctic ice sampling sites including Neumayer Station, where also aerosol filters were collected (<http://maps.grida.no/go/graphic/antarctica-topographic-map>).

them to Al_2O_3 or BeO , which can then be used as target material for the AMS measurement. Details of the aerosol sample preparation procedures have been described in Auer et al. (2007). In brief, for aerosol samples, ^{26}Al (together with ^{27}Al) and ^{10}Be were extracted from the filter matrix by leaching with HCl followed by ion exchange separation of ^{10}Be and ^{26}Al . The quantity of stable ^{27}Al in the extract was determined at a typical uncertainty of 3 to 4% by Atomic Absorption Spectrometry (AAS). While no Al carrier was added, up to 1 mg ^9Be was added at the start of the leaching procedure.

For the preparation of surface firn and drill chip ice samples, ^{26}Al and ^{10}Be had to be extracted from 5 to 10 kg samples, with a minimal loss of both isotopes. After melting the ice samples in polyethylene bags, which were pre-conditioned with HCl to avoid surface absorption of Al or Be, the melt water was acidified to pH 1 with HCl and spiked with carrier solutions containing 1 mg Be and 1 mg Al. Drill chip samples from the EDML ice core were heavily contaminated with drilling fluid (Exxol D40), which was separated from the sample prior to chemical processing. This was done as far as possible by gravitational separation of the melt water sample. The measured concentrations of ^{26}Al and ^{10}Be in the drilling fluid were below the detection limit, therefore the fluid is not a source of contamination. An additional ion exchange step was added to the chemical clean up procedure of these samples for the removal of the relatively abundant iron contamination. With these modifications of the chemical extraction procedure, efficiencies, similar to those for ice not contaminated by drilling fluid, were achieved. The measurements on the drill chip samples were also a first test of the suitability of ^{26}Al and ^{10}Be measurement for this core material.

The melt water from all ice samples was filtered through 0.45 µm pore size membrane filters prior to concentration. Concentration was either done by a rotary evaporator or by adsorption of Al and Be on a cation exchange resin (Biorad AG50 W-X8) from which they were eluted with 100 ml 6 M HCl. Since some of the samples already contained ^{27}Al , the content of ^{27}Al was quantified by AAS prior to addition of ^{27}Al carrier. The extract thus produced was further processed in the same way as the aerosol samples (Auer et al., 2007).

2.4. AMS measurement of ^{26}Al and ^{10}Be at VERA

^{26}Al and ^{10}Be measurements were performed at the Vienna Environmental Research Accelerator (VERA) of the University of Vienna, an AMS facility based on a 3 MV pelletron tandem accelerator. Details of the set-up and performance of VERA for $^{26}\text{Al}/^{27}\text{Al}$ and $^{10}\text{Be}/^9\text{Be}$ ratio

measurements are described elsewhere (Wallner et al., 2000; Auer et al., 2007; Priller et al., 2004; Michelmayr, 2007). A major obstacle for AMS measurement of ^{26}Al in environmental samples is the low efficiency for producing Al^- ions in the Cs-beam sputter ion source of the AMS system. $^{26}\text{Al}^-$ is used rather than ten the times more abundant $^{26}\text{Al}^{16}\text{O}^-$ ions, because ^{26}Mg does not form negative ions allowing for complete suppression of this isobaric interference. At VERA the overall efficiency (defined by the number of ^{26}Al atoms detected relative to their total number in an unprocessed sample) is typically 0.02%. ^{26}Al concentrations range between 5×10^4 and 10×10^4 atoms/kg in most of our ice samples, hence for a precision of 10% (achieved at approximately 100 counted ^{26}Al atoms), a minimum weight for ice samples of around 5 kg is required. Blank values of the $^{26}\text{Al}/^{27}\text{Al}$ ratio for pure chemical Al_2O_3 ranged between 0.4×10^{-15} to 1.5×10^{-15} , $^{26}\text{Al}/^{27}\text{Al}$ ratios between 0.8×10^{-15} and 1.5×10^{-15} were measured for blanks which underwent the chemical processing procedures. Blank values of the individual measurements are shown in Appendix A.

3. Results and discussion

3.1. Aerosol samples

Fig. 2 shows the atmospheric $^{26}\text{Al}/^{10}\text{Be}$ ratios measured from 47 aerosol samples. All data of aerosol sample measurements as well as of ice sample measurements are provided in Appendix A. The data indicate that the atmospheric $^{26}\text{Al}/^{10}\text{Be}$ ratio is constant with a mean of $(1.89 \pm 0.05) \times 10^{-3}$ (weighted mean \pm standard deviation of the mean, the $^{26}\text{Al}/^{10}\text{Be}$ ratio is throughout reported as the atomic ratio). The uncertainty of the ratios, which is on average 14%, is dominated by the AMS counting statistics of the ^{26}Al measurement. The reduced Chi-square (i.e. Chi-square divided by the number of degrees of freedom) of the data set is 0.87, indicating that the scattering of the data is dominated by the measurement uncertainties. Contrary to this finding, our previously published data set of atmospheric $^{26}\text{Al}/^{10}\text{Be}$ ratios contained a sequence of five samples from Sonnblick with a seemingly significant systematic variation of the $^{26}\text{Al}/^{10}\text{Be}$ ratio (Auer et al., 2007). Further analysis indicated however, that this variation was caused by a systematic error of the stable Al measurement, due to a matrix effect in the AAS measurement which was detected only recently. Four of these samples could be re-measured with a ratio not different from the atmospheric mean. These previous measurements have therefore been discarded and replaced by the re-measured data.

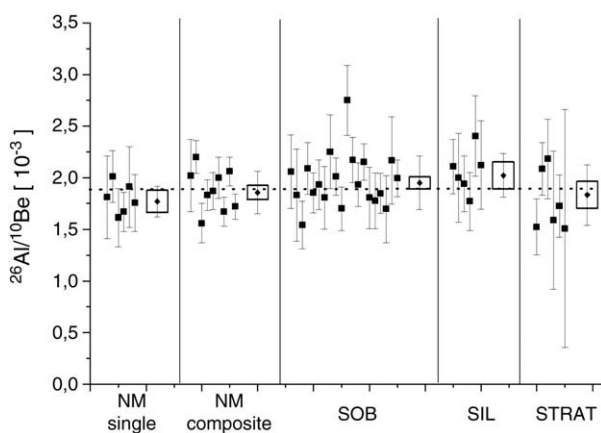


Fig. 2. Atmospheric $^{26}\text{Al}/^{10}\text{Be}$ ratios measured in aerosol filter samples including: Neumayer (NM) single filters and composite filter samples covering each 7 to 14 days and 6 months, respectively, Sonnblick (SOB), Schauinsland (SIL) and from an aircraft sampling campaign in Sweden (STRAT). The weighted mean of all atmospheric $^{26}\text{Al}/^{10}\text{Be}$ ratio measurements (1.89×10^{-3}) is indicated by the dotted line. Diamonds denote the weighted mean of each sample group, the uncertainty of the mean and the 1 sigma standard deviation are given by the box boundaries and uncertainty bars, respectively.

The generally good agreement of the data obtained from largely different aerosol bodies with the overall mean atmospheric ratio shows that the influence of non-atmospheric sources on the atmospheric $^{26}\text{Al}/^{10}\text{Be}$ ratio is relatively small. A possible influence of re-suspended meteoric and in situ produced ^{26}Al and ^{10}Be should be revealed by a correlation of the $^{26}\text{Al}/^{10}\text{Be}$ ratio with the stable Al concentration, since the latter may serve as proxy for mineral dust. For the samples from Sonnblick and Schauinsland, which are sites with mineral dust levels typical for mid latitudes. Stable Al concentrations change by a factor of 30 (data are provided in Appendix A), but no correlation with the $^{26}\text{Al}/^{10}\text{Be}$ ratio was observed ($r = 0.034$). For the stratospheric and Neumayer samples stable Al concentrations were below the analytical detection limit. It is also noteworthy, that no significant correlation between the concentrations of ^{26}Al or ^{10}Be with stable Al was observed (Fig. 3). Our results suggest that in situ produced and re-suspended ^{26}Al or ^{10}Be can be neglected for the mid-latitude Schauinsland and Sonnblick sites, which implies also no effect for the Antarctic and stratospheric samples, characterized by much lower mineral dust levels. These findings are supported by the similar mean ratios measured in the samples from the northern hemispheric sampling sites $(1.96 \pm 0.07) \times 10^{-3}$ and in the Antarctic aerosol samples $(1.84 \pm 0.05) \times 10^{-3}$, respectively. A Student-*t* test of the two data sets yields a two-tailed *p* value of 0.061 indicating that the difference between the two means is not clearly significant.

Also the aerosol filters from the high altitude flight sampling campaign in Sweden have a mean $^{26}\text{Al}/^{10}\text{Be}$ ratio not significantly different from tropospheric values, but with $(1.83 \pm 0.14) \times 10^{-3}$, clearly lower than the ratio of $(3.8 \pm 0.6) \times 10^{-3}$ reported by Raisbeck et al. (1983) from measurements of two stratospheric aerosol filters. Our filters were sampled at 12.5 km altitude, close to the tropopause, so they might have collected aerosol from the upper troposphere rather than from the stratosphere. The high ^{10}Be concentrations of $(3.05 \pm 0.23) \times 10^6$ atoms/ m^3 (mean \pm standard deviation) are however strongly indicative of stratospheric air. They exceed the overall mean of $(6.9 \pm 3.4) \times 10^4$ atoms/ m^3 from Sonnblick and Schauinsland by almost a factor of 50 and agree very well with 3×10^6 atoms/ m^3 reported by Jordan et al. (2003), for the lower stratosphere determined in several flight sampling campaigns. Concluding, our aircraft samples seem to be a good representation of lower stratospheric air of the mid latitudes.

The lack of vertical variation of the $^{26}\text{Al}/^{10}\text{Be}$ ratio seems to be at odds with the expected decrease of the production ratio with increasing atmospheric depth. However, since the ^{26}Al and ^{10}Be concentrations measured at the ground level sites are a mixture of tropospheric and stratospheric air, the $^{26}\text{Al}/^{10}\text{Be}$ ratio may lie between the pure stratospheric and the pure tropospheric values. We used a two-box model for the atmosphere to investigate the effect of atmospheric

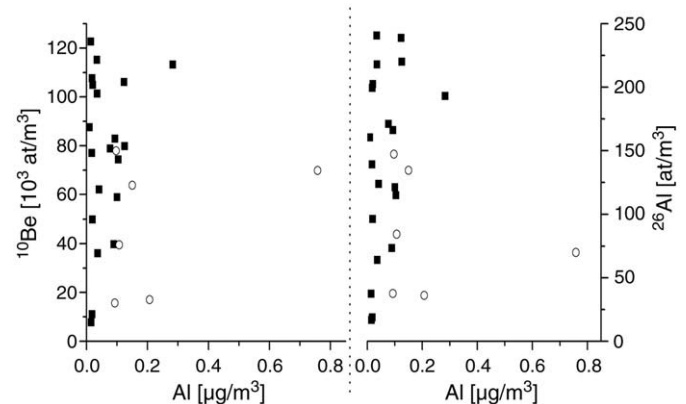


Fig. 3. ^{26}Al and ^{10}Be versus stable Al concentrations in aerosol filters from Sonnblick (squares) and Schauinsland (open circles). Stable Al is here used as an indicator for eolian mineral dust. The mean uncertainties are 8% for the Al concentration, 7% for the ^{10}Be concentration and 15% for the ^{26}Al concentration.

mixing on the $^{26}\text{Al}/^{10}\text{Be}$ ratio. For comparison with our measurements, high latitudes (60 to 90°) were treated separately from mid latitudes (30 to 60°). Input data for the two-box model are the altitude and latitude dependent atmospheric production rates based on the model by Masarik and Beer (1999). Production rates from this model were available in 30 g/cm² atmospheric depths and 10° latitude intervals (Beer, pers. comm.). From this data we calculated the mean $^{26}\text{Al}/^{10}\text{Be}$ production ratios for the stratosphere, the troposphere and for the whole atmosphere separately. As this calculations shows, the expected $^{26}\text{Al}/^{10}\text{Be}$ ratio for a completely mixed atmosphere is close to the value in a well mixed stratosphere (see Table 2), which is a consequence of the up to 10 times higher production in the stratosphere, relative to the troposphere. Consequently the lack of a significant difference between stratospheric and tropospheric $^{26}\text{Al}/^{10}\text{Be}$ ratios can be explained by a sufficient mixing between the stratosphere and troposphere.

The two-box-model calculations further indicate that even a relatively weak contribution of stratospheric air to the measured signal produces a $^{26}\text{Al}/^{10}\text{Be}$ ratio which is close to the stratospheric one. For example reducing the stratospheric input into the troposphere by a factor of 2 would reduce the tropospheric $^{26}\text{Al}/^{10}\text{Be}$ ratio by only 4.5% relative to a completely mixed atmosphere. Consequently, a significant decrease of the $^{26}\text{Al}/^{10}\text{Be}$ ratio is only achieved by a very strong decoupling of the stratosphere from the troposphere. Nevertheless, such an effect appears to be visible in the semi-annual data from the Neumayer station (NM composite). These data indicate a positive correlation of the $^{26}\text{Al}/^{10}\text{Be}$ ratio with the ^{26}Al as well with the ^{10}Be concentrations (Fig. 4), both having much higher concentrations in the stratosphere compared to the troposphere. Also visible in these data is a seasonal trend with lower $^{26}\text{Al}/^{10}\text{Be}$ ratios in the July to December period (mean $^{26}\text{Al}/^{10}\text{Be} = (1.72 \pm 0.08) \times 10^{-3}$) relative to January to June (mean $^{26}\text{Al}/^{10}\text{Be} = (2.02 \pm 0.08) \times 10^{-3}$). As measurements of the $^{10}\text{Be}/^7\text{Be}$ ratio in aerosol samples from Neumayer (Wagenbach, 1994) indicate, the former period is characterized by a generally weaker stratospheric influence, while the maximum stratospheric fraction is seen between January and June. Following our two-box model calculations, the observed difference between the two means could be explained by reducing the stratospheric input by a factor of five, relative to a completely mixed atmosphere. However, on longer time scales, which is relevant for ice samples covering several years, such effects are expected to be compensated, as indicated by the fact that the difference between the $^{26}\text{Al}/^{10}\text{Be}$ ratios at Neumayer and the European samples could not be shown to be clearly significant. Assuming, however, that the difference is due to atmospheric mixing and not a statistical variation, our data indicate, that the $^{26}\text{Al}/^{10}\text{Be}$ ratio may systematically deviate up to 3% from the atmospheric mean ratio at a given sampling site.

For the assessment of the extraterrestrial ^{26}Al fraction we measured ^{53}Mn in aerosol samples from Sonnblick and Neumayer as well as in a surface ice sample from Kohnen Station (Dronning Maud Land, Antarctica). The measurements of ^{53}Mn have been carried out at the AMS facility of the Munich MP tandem laboratory, following the method described by Knie et al. (2000). The mean atmospheric atomic ratio

Table 2

Calculated mean $^{26}\text{Al}/^{10}\text{Be}$ production ratio in the stratosphere and troposphere in mid (30°–60°) and high (60°–90°) latitudes, based on the isotope production rate model by Masarik and Beer (1999) for a mean tropopause height of 210 g/cm² and 270 g/cm² for mid latitudes and high latitudes, respectively. The relative stratospheric and tropospheric contributions to the overall ^{26}Al production are given in addition.

	Latitude 30°–60°		Latitude 60°–90°	
	$^{26}\text{Al}/^{10}\text{Be} \times 10^{-3}$	^{26}Al production (%)	$^{26}\text{Al}/^{10}\text{Be} \times 10^{-3}$	^{26}Al production (%)
Stratosphere	2.4	80	2.5	90
Troposphere	1.6	20	1.8	10
Stratosphere plus Troposphere	2.3		2.3	

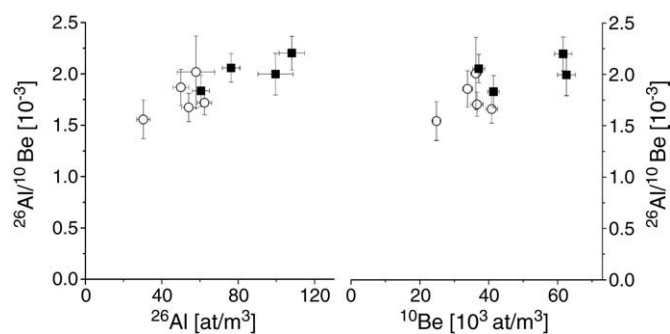


Fig. 4. $^{26}\text{Al}/^{10}\text{Be}$ ratios versus ^{26}Al and ^{10}Be concentrations in aerosol filters from Neumayer (“NM composite”) sampled from July 2000 to Dec 2004. Each of the data point represents filters covering a period of 6 months. July–Dec. open circles, Jan–Jun. squares.

($^{26}\text{Al}/^{53}\text{Mn}$)_{atm} is 0.106 (+0.063, −0.037). Based on production rates of ^{26}Al and ^{53}Mn in meteorites and interplanetary dust (Reedy, 1990; Nishiizumi et al., 1995; Michel, 1999) we have estimated the $^{26}\text{Al}/^{53}\text{Mn}$ atomic ratio in extraterrestrial matter to ($^{26}\text{Al}/^{53}\text{Mn}$)_{ext} = 0.26. Taking the extraterrestrial ^{26}Al fraction f_{ext} of the total atmospheric ^{26}Al as:

$$f_{\text{ext}} = (^{26}\text{Al}/^{53}\text{Mn})_{\text{ext}} / (^{26}\text{Al}/^{53}\text{Mn})_{\text{atm}}$$

we arrive at $f_{\text{ext}} = 0.028$ (+0.016, −0.010), with ($^{26}\text{Al}/^{53}\text{Mn}$)_{atm} = ($^{26}\text{Al}_{\text{ext}} + ^{26}\text{Al}_{\text{atm}}$) / ($^{53}\text{Mn}_{\text{ext}} + ^{53}\text{Mn}_{\text{atm}}$), where $^{26}\text{Al}_{\text{ext}}$, $^{26}\text{Al}_{\text{atm}}$, $^{53}\text{Mn}_{\text{ext}}$ and $^{53}\text{Mn}_{\text{atm}}$ are the atmospheric and extraterrestrial source terms and $^{53}\text{Mn}_{\text{atm}} = 0$. Thus, we may conclude that the contribution of extraterrestrial ^{26}Al to the total ^{26}Al budget is relatively small and thus not likely to significantly change the $^{26}\text{Al}/^{10}\text{Be}$ ratio.

3.2. ^{26}Al and ^{10}Be in Antarctic firm samples

The surface firm samples from the Antarctic sampling locations at Dome C and Kohnen are characterized by low precipitation rates, while the coastal sampling sites at Neumayer and Cap Prudomme have high precipitation rates. The seven samples from Dome C have a mean $^{26}\text{Al}/^{10}\text{Be}$ ratio of $(1.74 \pm 0.18) \times 10^{-3}$, the sample from Kohnen (DML) has a ratio of $(1.70 \pm 0.23) \times 10^{-3}$. The four samples from Cap Prudomme and Neumayer, respectively, have mean ratios of $(1.62 \pm 0.36) \times 10^{-3}$ and $(0.96 \pm 0.45) \times 10^{-3}$. Within the analytical uncertainties the firm values of the $^{26}\text{Al}/^{10}\text{Be}$ ratio are indistinguishable.

The $^{26}\text{Al}/^{10}\text{Be}$ ratios measured in the Dome C and Kohnen firm samples are, within the uncertainty, in good agreement with the average atmospheric $^{26}\text{Al}/^{10}\text{Be}$ ratio. This suggests that the air firm transfer (and its spatio-temporal variability) has no detectable influence on the $^{26}\text{Al}/^{10}\text{Be}$ ratio in surface firm. Therefore, under the assumption, that this also applies to glacial conditions, this basic requirement for $^{26}\text{Al}/^{10}\text{Be}$ dating is fulfilled. Our inland firm data are also in good agreement with the recently published $^{26}\text{Al}/^{10}\text{Be}$ ratio of $(1.75 \pm 0.19) \times 10^{-3}$ measured in two approx. 1500 years old firm samples from Dome Fuji (East Antarctica) (Horiuchi et al., 2007), and similar to an earlier published ratio of $(2.20 \pm 0.36) \times 10^{-3}$ determined from two Antarctic ice samples in the Yamato and Thiel mountains, respectively (Middleton and Klein, 1987).

Based on the ^{26}Al concentrations in the firm samples, the deposition flux of ^{26}Al is obtained, by multiplying concentrations with the accumulation rate, which may be compared to model calculations of the atmospheric ^{26}Al production rate (Table 3). However, the calculated ^{26}Al production rate has a relatively high uncertainty, since only few data on cross sections for the production of ^{26}Al from argon are available (Kubo, 2001; Reyss et al., 1981). ^{10}Be production rates are known with higher accuracy. Therefore, instead of using calculated ^{26}Al production rates, we have used the ^{10}Be data from the Masarik and Beer (1999) model and multiplied them with the overall mean atmospheric $^{26}\text{Al}/^{10}\text{Be}$ ratio determined in this work. This gives a global mean atmospheric ^{26}Al

Table 3

Average measured concentrations and ^{26}Al and ^{10}Be deposition flux at various Antarctic sampling sites and calculated production rates for ^{26}Al and ^{10}Be .

	^{10}Be (10^3 at./g)	^{26}Al (at./g)	$^{10}\text{Be}^1$ (10^4 at./cm 2 a)	$^{26}\text{Al}^1$ (at./cm 2 a)
Neumayer	11.2 ± 0.8	12 ± 8	40 ± 3 ²	460 ± 290 ²
Cap Prudomme	12.7 ± 0.9	19 ± 9	3	3
Kohnen	30.2 ± 1.1	52 ± 7	19 ± 1	330 ± .50
Dome C	55.6 ± 4.1	102 ± 7	14 ± 2	250 ± 20
<i>Production rates</i>				
Polar atmosphere (90°–60°)			121	2340
Polar troposphere			17	230
Polar stratosphere			103	2110
Global atmosphere				1280

¹Total deposition has been calculated using the accumulation rates given in.

²Lower limit from mainly fresh snow including almost no dry deposition flux.

³No flux given for Cap Prudomme due to unknown accumulation rate.

production rate of 1280 atoms $\text{cm}^{-2} \text{a}^{-1}$. The observed values are up to one order of magnitude below the respective production rates in the polar atmosphere. This imbalance requires a substantial export out of the Antarctic continent. As discussed by Wagenbach et al. (1998), a net outflow of aerosol produced within the central polar cell is expected due to the rather long atmospheric residence time there, compared to lower latitudes. Our observed fluxes from Antarctica (which, moreover, depend to first order linearly on the local accumulation rate) are thus a poor representation of the respective atmospheric production rates.

3.3. The $^{26}\text{Al}/^{10}\text{Be}$ ratio in deep Antarctic ice

From our measurements of the atmospheric $^{26}\text{Al}/^{10}\text{Be}$ ratio in aerosol from various air masses and in firn samples, we may conclude that this ratio is dominated by atmospheric production, while extraterrestrial and terrestrial ^{26}Al sources as well as re-suspension of ^{26}Al and ^{10}Be play a minor role. Also the vertical and latitudinal gradients in the production rates exert only a minor influence. Our measurements constrain the temporal and geographical variation of the $^{26}\text{Al}/^{10}\text{Be}$ ratio to less than 5% around the atmospheric value of 1.89×10^{-3} . In addition, it is confirmed that the air/firn transfer does not change the $^{26}\text{Al}/^{10}\text{Be}$ ratio to any measurable extent. Thus the basic prerequisites for deploying the $^{26}\text{Al}/^{10}\text{Be}$ chronometer appear to be met, justifying our attempt for a pilot study of $^{26}\text{Al}/^{10}\text{Be}$ in the lower part of the EPICA-EDML ice core.

As shown in Fig. 5, the most outstanding feature of the ice core data is a pronounced $^{26}\text{Al}/^{10}\text{Be}$ peak made up of several consecutive samples between 2580 and 2593 m depth. So far no other samples showed such a large and systematic elevation above the mean atmospheric $^{26}\text{Al}/^{10}\text{Be}$ ratio. By linear extension of the age-depth relation

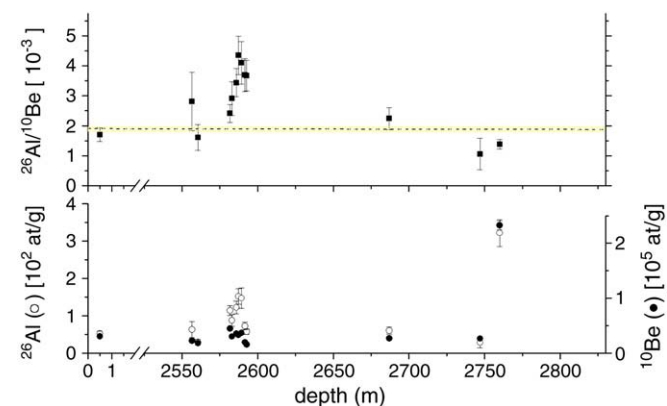


Fig. 5. Depth profile of the $^{26}\text{Al}/^{10}\text{Be}$ ratio (upper panel) and of ^{26}Al and ^{10}Be concentrations (lower panel) in the bottom part of the Antarctic EPICA DML ice core. The dotted line corresponds to the overall mean atmospheric $^{26}\text{Al}/^{10}\text{Be}$ of 1.89×10^{-3} .

established by Ruth et al. (2007), we may expect that this section of the core corresponds to a time interval of several thousand years. The samples in question have been measured in two independent series, with self-contained sample preparation and AMS set-up, which makes a systematic measurement error unlikely.

Among natural processes that could potentially be responsible for this anomaly in the isotope ratio, concentration changes in the final stage of ice sample development cannot be excluded. For example, strong enhancements of ^{10}Be , which exceeded concentrations in adjacent samples by one order of magnitude, have been detected in the Dome C ice core by Raisbeck et al. (2006) at a depth of approx. 150 to 100 m above bedrock. These spikes, observed in samples over a relatively short interval of 11 cm, cannot be explained by production rate changes, but are due to yet an unknown concentration process operating on a short length scale. If such an effect acts differently on the two isotopes, the resulting fractionation may produce the observed effect. It is noted however, that the high isotope ratios in the EDML core are observed continuously over a length of more than 10 m, a much wider depth range than the elevated ^{10}Be levels in Dome C. Furthermore, no unusually high ^{10}Be concentrations were observed in this section of the EDML core. As shown in Fig. 6, the higher $^{26}\text{Al}/^{10}\text{Be}$ ratio is concurrent with a significant enhancement of ^{26}Al , but with almost no enhancement of ^{10}Be . Potential additional contribution of ^{26}Al could originate either from stratospheric production, from an extraterrestrial source or from terrestrial dust. The stratospheric $^{26}\text{Al}/^{10}\text{Be}$ production ratio is not high enough to explain the observed peak by changes in vertical mixing of air. The $^{26}\text{Al}/^{10}\text{Be}$ production ratio can also be altered by strong changes of the cosmic ray energy spectrum, however no such changes can be inferred over the last 10^7 years (Michel et al., 1996). To explain the $^{26}\text{Al}/^{10}\text{Be}$ peak by an increased input of extraterrestrial material, would require an extraterrestrial ^{26}Al flux equal to the atmospheric production. This scenario would entail an increase of the extraterrestrial ^{26}Al input in the peak period by at least a factor of 20 (according to our estimate of the present extraterrestrial ^{26}Al fraction of around 5%) which seems unlikely: Estimates of past accretion of extraterrestrial matter indicate either a stable mass flux during the last 30 ka (Winkler and Fischer, 2006) or changes during the last 450 ka but not larger than a factor of 3.5 (Farley and Patterson, 1995). Whether short term fluctuations of the extraterrestrial mass flux could cause such a high variation can currently not be answered.

In order to check for a contribution of re-suspended or in situ produced ^{26}Al , we used concentrations of non-sea-salt calcium in the EDML ice core (H. Fischer pers. comm.) as proxy for mineral dust. However, neither extraordinarily high mineral dust levels, nor a significant correlation of non-sea-salt calcium with $^{26}\text{Al}/^{10}\text{Be}$ was observed. Presently, we can give no conclusive explanation for the significant enhancement of ^{26}Al , leading to a correspondingly high $^{26}\text{Al}/^{10}\text{Be}$ ratio.

A further outstanding feature in the EDML data set is the sharp rise in ^{10}Be and ^{26}Al concentrations in the lowest samples, at 2760 m depth.

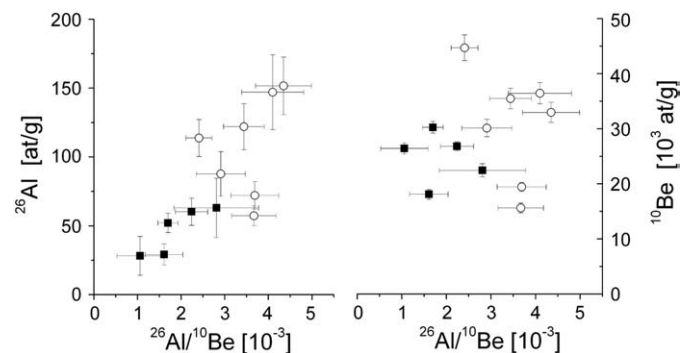


Fig. 6. $^{26}\text{Al}/^{10}\text{Be}$ ratio versus ^{26}Al and ^{10}Be concentrations in the samples from 2554 to 2748 m depth of the EDML ice core. Data from the section between 2580 and 2593 m depth are shown as open circles.

Relative to the average, ^{10}Be increases by a factor of 10 and ^{26}Al by a factor of 5. This concentration increase is too large to be caused by increased production or reduced accumulation (which should be seen in other dust components as well). The rise is similar to the ^{10}Be peak concentrations observed in the EPICA Dome C core by Raisbeck et al. (2006), however the peak in the EDML sample is measured over a one meter sample length, a much more extended depth range than the Dome C ^{10}Be peaks. The proximity of this sample to the bedrock (the distance is approximately 20 m) supports the suggestion by Raisbeck et al. (2006), that the perturbations may be caused by an internal concentration effect, caused by a mechanism that is not yet understood.

3.4. Implications for the $^{26}\text{Al}/^{10}\text{Be}$ chronometer

The variation of the $^{26}\text{Al}/^{10}\text{Be}$ ratio in the EDML ice core are clearly larger than we observed in the atmospheric and surface ice samples, though each core sample covers several orders of magnitudes longer time intervals. Firstly, a significant, and so far unexplained, increase of the $^{26}\text{Al}/^{10}\text{Be}$ ratio has been observed, which brings into question the assumption that the $^{26}\text{Al}/^{10}\text{Be}$ ratio has been exclusively changed by radioactive decay. Furthermore, a concurrent nearly ten-fold increase of ^{10}Be and ^{26}Al just near bedrock points to internal processes in that particular core section. Since the EDML core approaches its pressure melting point in the investigated section, premelting is strongly favoured (Dash et al., 2006). Although this process acts on the grain scale, Rempel and Wettlaufer (2003) predicted that perturbations of soluble impurities may occur over a distance of up to 50 cm. Indeed Kaufmann (2008) reported a strong desalination in the bottom of the EDML core starting at a depth of 2770 m, which is attributed to a downward movement of the intergrain liquid layer. In conclusion, the few combined ^{26}Al and ^{10}Be data do not allow judging the reason for the observed isotope anomalies, but there is ample evidence, that the relatively warm bottom layer of Antarctic ice cores allows perturbation and mobilisation of impurities preserved in the ice matrix.

Disregarding for the moment these indications of potential causes for variations of the $^{26}\text{Al}/^{10}\text{Be}$ ratio, other than the radioactive decay, the two lowest core samples are used for a hypothetical dating. The $^{26}\text{Al}/^{10}\text{Be}$ ratio in these samples is, within the uncertainty, significantly lower than the atmospheric average. Under the assumptions, that the elevated $^{26}\text{Al}/^{10}\text{Be}$ ratio in the higher part of the EDML core can be regarded as an exceptional event, and that the substantially increased ^{26}Al and ^{10}Be concentrations in the bottom sample are not accompanied by a fractionation between these isotopes, the age of the two lowest samples can be calculated. Using the mean atmospheric ratio of 1.89×10^{-3} as the ratio of deposited ^{26}Al and ^{10}Be , the $^{26}\text{Al}/^{10}\text{Be}$ ratio $(1.38 \pm 0.17) \times 10^{-3}$ of the deepest sample (depth 2760 m) would give a nominal $^{26}\text{Al}/^{10}\text{Be}$ age of $(6.7 \pm 2.6) \times 10^5$ a. The adjacent sample (around 15 m above at 2746–2748 m), which does not have anomalous concentration levels, provides a ratio of $(1.06 \pm 0.53) \times 10^{-3}$, also below the mean atmospheric ratio. The uncertainty of the age estimate of $(1.2 \pm 1.0) \times 10^6$ a for this sample is large though, due to the low precision of the ^{26}Al measurement.

Based on the data of the drill chip measurements reported here, the precision to which single ice samples can be dated with the $^{26}\text{Al}/^{10}\text{Be}$ chronometer can be estimated. Fig. 7 shows the relative uncertainty expected for a 7 kg and 14 kg sample size, respectively, and taking radioactive decay into account. The estimate is based on the mean atmospheric $^{26}\text{Al}/^{10}\text{Be}$ ratio of 1.89×10^{-3} , with an uncertainty of 5% and an average analytical uncertainty for the EDML samples of 14%. The absolute dating uncertainty increases with age due to radioactive decay, however the relative uncertainty reaches a flat minimum in the order of 30–40% for samples which are 1 to 3 million old. Since this relatively large uncertainty is to a large part due to the combination of low ^{26}Al concentrations and a low measurement efficiency, improvements of the uncertainty could mainly be achieved by increasing the measurement efficiency.

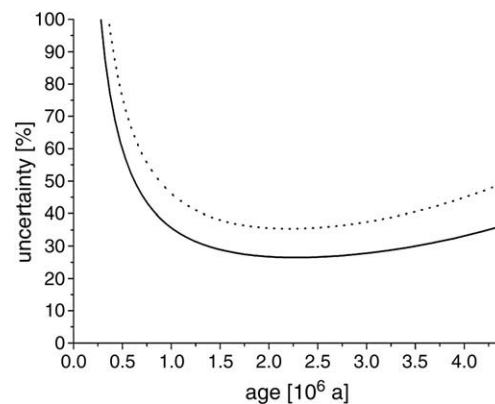


Fig. 7. Expected ice dating uncertainty via the $^{26}\text{Al}/^{10}\text{Be}$ ratio, adopting a mean analytical uncertainty of 14% for recent samples and a sample mass of 7 kg (dotted line) and 14 kg ice (straight line), respectively.

4. Conclusions

The $^{26}\text{Al}/^{10}\text{Be}$ ratio measured in various atmosphere aerosol samples from both hemispheres is found to be constant at 1.89×10^{-3} within 5% and does not significantly differ from the value seen in Antarctic surface firn. Supported by mineral dust analyses, these observations indicate a minor influence of in situ produced or re-suspended ^{26}Al to the atmospheric $^{26}\text{Al}/^{10}\text{Be}$ ratio as well as no significant impact of the stratosphere/troposphere exchange. Measurement of ^{53}Mn in atmospheric and ice samples further indicates that extraterrestrial ^{26}Al exerts a negligible contribution to the overall atmospheric ^{26}Al . Also, the transfer from air to firn does not seem to influence the $^{26}\text{Al}/^{10}\text{Be}$ ratio, as revealed by firn measurements. The finding of a rather constant initial $^{26}\text{Al}/^{10}\text{Be}$ value in aerosol and firn supports the basic use of this ratio as a chronometer in suitably old archives derived from atmospheric deposition, such as glacier ice.

First $^{26}\text{Al}/^{10}\text{Be}$ ratio analyses in a deep Antarctic ice core showed much higher variability than what may be expected from recent atmospheric values or radioactive decay. In addition, a strong concentration enhancement of both isotopes in the bottom sample close to bedrock has been observed. Thus, the requirement that the $^{26}\text{Al}/^{10}\text{Be}$ ratio be exclusively changed by radioactive decay might become questionable in the basal layer of the Antarctic ice sheet, where the ice melting point may be approached, accompanied by an increased mobility of the ice impurities. This observation calls for a detailed study of the behaviour of impurities in the ice body to be dated by the $^{26}\text{Al}/^{10}\text{Be}$ ratio, as well as more dedicated $^{26}\text{Al}/^{10}\text{Be}$ analyses in near bedrock ice. Nevertheless, radiometric $^{26}\text{Al}/^{10}\text{Be}$ dating remain promising, especially in constraining the age of potentially very old ice (Schäfer et al., 2000; Sugden et al., 1995). It would be very useful if alternative experimental methods on the horizon, like dating via the ^{40}Ar concentration in the ice [Bender et al., 2008], turn also out to be feasible.

Acknowledgements

The authors would like to express their gratitude to Susanne Preunkert and co-workers (LGGE) for sampling the Cap Prudomme ice as well as to Herbert Gohla (CTBTO, Austria) and Gerhard Schauer (ZAMG, Austria) for providing aerosol samples from the Sonnblick Observatory and Dr. Lars-Erik de Geer (FOI, Sweden) for providing stratospheric aerosol filters from Sweden. We also thank two anonymous reviewers for their helpful suggestions. This work was funded by the Austrian Science Foundation (FWF), project number P17442-N02. This work is a contribution to the European Project for Ice Coring in Antarctica (EPICA), a joint European Science Foundation/European Commission scientific programme, funded by the EU and by national contributions from Belgium, Denmark, France, Germany, Italy, the Netherlands, Norway, Sweden, Switzerland and the United Kingdom. This is EPICA publication no. 236.

Appendix A. Sample analysis results

Aerosol filter measurements																					
Sample name	²⁶ Al/ ¹⁰ Be		²⁶ Al		¹⁰ Be		Al carrier		Stable Al		Be carrier		²⁶ Al AMS measurement			¹⁰ Be AMS measurement			Sample size (m ³ air)	Sampling start (Date)	Sampling time (days)
	Ratio (10 ⁻³)	+/- (%)	Conc. (10 ⁻³ at/m ³)	+/- (%)	Conc. (10 ⁶ at/m ³)	+/- (%)	(mg/sample)	(mg/sample)	+/- (%)	(mg/sample)	+/- (%)	²⁶ Al/ ²⁷ Al (×10 ⁻¹⁵)	+/- (%)	blank (×10 ⁻¹⁵)	¹⁰ Be/ ⁹ Be (×10 ⁻¹²)	+/- (%)	blank (×10 ⁻¹⁴)				
<i>Neumayer single</i>																					
Al_NM92_04	1.81	21.9	80.1	21.5	44.3	4.5	1	1.00	4	1	4	44.6	21.1	1.3	8.22	2.2	2.60	12,417	25.4.1992	14	
Al_NM93_06	2.01	12.1	128.4	11.4	63.9	4.3	1	1.00	4	1	4	43.3	10.6	1.3	7.18	1.6	2.60	7520	27.3.1993	7	
Al_NM93_30	1.61	17.1	75.5	16.5	46.8	4.2	1	1.00	4	1	4	29.9	16.1	1.3	6.18	1.4	2.60	8838	21.11.1993	14	
Al_NM95_12	1.67	10.8	109.2	10.0	65.4	4.2	1	1.00	4	1	4	38.2	9.2	1.3	7.62	1.2	2.60	7806	28.3.1995	7	
Al_NM95_21	1.91	20.2	23.2	19.6	12.1	4.7	1	1.00	4	1	4	13.0	19.2	1.3	2.27	2.4	2.60	12,513	4.7.1995	13	
Al_NM95_24	1.75	15.3	44.7	14.7	25.5	4.3	1	1.00	4	1	4	24.0	14.2	1.3	4.56	1.5	2.60	11,966	2.8.1995	13	
<i>Neumayer composite</i>																					
NMPool_2_00	2.02	17.4	57.9	16.9	28.7	4.1	1	1.36	4.1	1	4	110.0	16.4	1.3	24.61	1.0	2.60	57,425	26.6.2000	182	
NMPool_1_01	2.20	7.5	108.0	6.2	49.1	4.1	1	1.19	4.1	1	4	214.0	4.7	1.3	38.59	0.9	2.60	52,590	25.12.2000	189	
NMPool_2_01	1.56	12.1	30.4	11.4	19.5	4.2	1	1.17	4.1	1	4	56.6	10.6	1.3	14.14	1.3	2.60	48,491	2.7.2001	182	
NMPool_1_02	1.83	8.4	60.5	7.4	33.0	4.1	1	1.12	4.9	1	4	128.9	5.5	1.3	26.32	1.0	2.60	53,380	31.12.2001	182	
NMPool_2_02	1.87	9.4	50.0	8.4	26.7	4.3	1	1.04	4.9	1	4	64.9	6.8	1.3	12.03	1.5	2.60	30,109	1.7.2002	182	
NMPool_1_03	2.00	10.2	99.5	9.3	49.9	4.2	1	1.03	4.9	1	4	124.7	7.9	1.3	21.46	1.2	2.60	28,808	13.1.2003	168	
NMPool_2_03	1.67	8.2	54.1	7.1	32.3	4.2	1	1.05	4.9	1	4	130.1	5.1	1.3	27.11	1.2	2.60	56,113	30.6.2003	224	
NMPool_1_04	2.06	7.5	76.2	6.1	37.1	4.4	1	1.02	4.1	1	4	167.2	4.5	1.3	27.77	1.9	1.60	50,133	9.2.2004	154	
NMPool_2_04	1.72	7.0	62.4	5.3	36.3	4.6	1	1.05	3.0	1	4	168.3	4.3	1.3	34.27	2.3	1.60	63,238	12.7.2004	182	
<i>Sonnblick</i>																					
S4+050503	2.06	17.4	121.1	16.6	58.9	5.1		0.49	3.5	0.5	4	54.1	16.3	0.4	8.50	3.2	2.60	4833	4.5.2003	2	
S9+100503	1.83	26.3	160.3	25.8	87.5	5.1		0.27	3.3	0.5	4	289.0	25.6	0.4	28.00	3.1	2.60	10,703	9.5.2003	2	
S23+250503	1.54	16.3	114.7	15.5	74.3	5.1		0.86	3.4	0.5	4	49.5	15.2	0.4	18.39	3.2	2.60	8279	23.5.2003	2	
S290503	2.09	13.2	240.6	12.1	115.2	5.1		0.75	4.1	1	4	114.0	11.4	0.4	13.71	3.1	2.60	7966	29.5.2003	1	
S300503	1.85	11.6	199.3	10.4	107.6	5.1		0.63	4.1	1	4	105.1	9.5	0.4	12.01	3.2	2.60	7467	30.5.2003	1	
S310503	1.93	13.5	202.4	12.5	104.9	5.1		0.65	3.8	1	4	109.0	11.9	0.4	12.23	3.2	2.60	7806	31.5.2003	1	
S010603	1.81	18.2	139.0	17.5	77.0	5.1		0.63	3.5	1	4	76.0	17.1	0.4	8.83	3.2	2.60	7677	1.6.2003	1	
S15+170603	2.25	18.2	238.7	17.5	106.0	5.1		1.21	3.1	0.5	4	87.0	17.2	0.4	31.26	3.1	2.60	9864	15.6.2003	2	
S240603	2.01	8.9	166.3	6.7	82.8	5.9		1.20	2.4	0.5	4	46.6	6.3	1.1	18.56	4.3	2.66	7500	24.6.2003	1	
S250603	1.70	12.1	193.0	10.6	113.2	5.8		2.62	5.4	0.5	4	24.8	9.2	1.1	25.38	4.2	2.66	7500	25.6.2003	1	
S260603	2.75	12.4	219.8	10.9	79.8	5.9		1.44	7.9	0.5	4	51.3	7.6	1.1	17.89	4.4	2.66	7500	26.6.2003	1	
S270603	2.17	10.0	171.2	8.1	78.8	5.9		1.08	5.2	0.5	4	53.3	6.2	1.1	17.67	4.3	2.66	7500	27.6.2003	1	
S040703	1.93	10.8	96.3	7.9	49.9	7.4		1.29	3.2	1	4	50.2	7.2	1.1	11.18	6.2	5.60	15,000	4.7.2003	1	
S050703	2.15	7.7	217.9	6.4	101.3	4.3		1.53	2.2	1	4	95.8	6.0	1.1	22.71	1.6	5.60	15,000	5.7.2003	1	
S290104	1.81	16.2	37.3	15.7	20.7	4.5		1.21	2.1	1	4	20.7	15.6	1.1	4.63	2.0	5.60	15,000	29.1.2004	1	
S160404	1.78	14.9	64.1	14.1	36.0	5.0		1.55	2.9	1	4	27.9	13.8	1.2	8.08	3.0	5.60	15,000	16.6.2004	1	
S170404	1.85	11.1	73.4	10.2	39.8	4.5		2.33	5.0	1	4	21.2	8.8	1.2	8.91	2.0	5.60	15,000	17.6.2004	1	
S180404	1.70	18.9	18.8	17.9	11.1	6.0		1.27	2.3	1	4	10.0	17.8	1.1	2.48	4.4	5.60	15,000	18.6.2004	1	
S190404	2.17	19.4	16.7	18.1	7.7	6.9		1.22	2.5	1	4	9.2	17.9	1.1	1.73	5.7	5.60	15,000	19.6.2004	1	
S200404	1.99	8.5	123.7	7.3	62.1	4.4		1.62	2.6	1	4	51.5	6.8	1.1	13.91	1.9	5.60	15,000	20.6.2004	1	
<i>Schauinsland</i>																					
SIL33_03	2.11	12.8	107.5	11.7	51.0	5.0		11.63	4.3	0.5	4	32.1	10.9	0.4	118.10	3.1	2.60	77,445	18.8.2003	7	
SIL06_06	2.40	16.2	37.6	15.6	15.6	4.5		0.78	4.6	0.40	4	18.8	14.9	0.4	5.11	2.2	0.84	8643	6.2.2003	7	
SIL08_06	2.12	20.3	36.1	16.8	17.0	11.4		0.86	2.1	0.39	11	16.2	16.7	0.4	5.60	3.2	0.84	8565	20.2.2003	7	
SIL19_03	2.00	21.6	147.2	18.9	73.5	10.6		6.06	4.4	0.73	10	8.7	18.4	0.4	12.10	2.1	0.84	7993	5.5.2003	7	
SIL27_03	1.94	14.1	84.3	12.0	43.5	7.5		0.75	4.1	0.73	7	40.8	11.3	0.4	7.25	3.6	0.84	8093	30.6.2003	7	
SIL38_03	1.77	15.9	109.6	9.9	61.9	12.5		1.63	2.0	0.73	12	23.8	9.7	0.4	10.04	2.8	0.84	7869	15.9.2003	7	

Stratospheric samples																				(minutes)
FO11	1.52	17.4	4450.7	52.7	2914.0	50.3	*	2.70	2.1	0.5	4	6.9	16.4	1.1	8.10	3.4	1.60	93	20.12.2004	30
FO12	2.08	11.9	6511.2	51.2	3118.4	50.2	*	3.08	2.5	0.5	4	8.8	10.5	1.1	8.67	2.8	1.60	93	20.12.2004	30
FO13	2.18	18.0	6937.8	53.0	3180.6	50.2	*	3.01	4.8	0.5	4	9.6	16.8	1.1	8.84	2.0	5.60	93	20.12.2004	30
FO14	1.59	41.9	5369.6	65.0	3378.5	50.3	*	3.35	2.1	0.5	4	6.7	41.6	1.1	9.39	3.5	5.60	93	20.12.2004	30
FO16	1.73	17.9	5101.7	52.9	2951.7	50.2	*	2.48	6.0	0.5	4	8.6	16.2	1.1	8.20	3.0	1.60	93	20.12.2004	30
FO17	1.51	76.5	4130.7	91.3	2738.1	50.2	*	2.80	6.8	0.5	4	6.2	76.1	1.1	7.61	2.2	5.60	93	20.12.2004	30

Firn and ice sample measurements																				
Name	²⁶ Al/ ¹⁰ Be		²⁶ Al		¹⁰ Be		Al carrier (mg)	Stable Al		Stable Be		²⁶ Al AMS measurement			¹⁰ Be AMS measurement			Sample size (kg)	Sample depth (m)	Sample length (m)
	Ratio (10 ⁻³)	+/- (%)	Conc. (at/g)	+/- (%)	Conc. (10 ³ at/g)	+/- (%)		(mg/sample)	+/- (%)	(mg/sample)	+/- (%)	²⁶ Al/ ²⁷ Al (×10 ⁻¹⁵)	+/- (%)	blank (×10 ⁻¹⁵)	¹⁰ Be/ ⁹ Be (×10 ⁻¹²)	+/- (%)	Blank (×10 ⁻¹⁴)			
<i>Dome C firn core</i>																				
A/DCFC1	1.68	25.3	80.0	24.8	47.6	5.2	1	1.00	4	1	4	10.4	24.5	1.2	2.06	3.3	3.28	2.9	0	4
A/DCFC2	1.59	17.5	104.8	16.8	65.8	4.9	1	1.00	4	1	4	11.7	16.3	1.2	2.46	2.8	3.28	2.5	4	4
A/DCFC3	1.40	18.0	102.9	17.4	73.6	4.5	1	1.00	4	1	4	18.4	16.9	1.2	4.40	2.1	3.28	4.0	8	4
<i>Dome C snow pit samples</i>																				
A/DCPit09_12	1.43	18.2	87.8	17.6	61.5	4.8	1	1.00	4	1	4	18.9	17.1	1.2	4.41	2.7	3.28	4.8	0.9	0.3
A/DCPit12_15	2.26	15.6	107.9	14.6	47.8	5.4	1	1.00	4	1	4	20.8	14.1	1.2	3.07	3.6	3.28	4.3	1.2	0.3
A/DCPit15_18	2.31	15.5	102.3	14.3	44.3	6.0	1	1.00	4	1	4	22.9	13.7	1.2	3.31	4.5	3.28	5.0	1.5	0.3
A/DCPit18_21	2.41	16.0	136.7	15.4	56.8	4.5	1	1.00	4	1	4	35.6	14.9	1.2	4.92	2.0	3.28	5.8	1.8	0.3
<i>Cap Prudhomme</i>																				
A/CP_A5	0.97	76.7	13.7	76.5	14.1	5.8	1	1.00	4	1	4	2.5	76.4	1.2	0.84	4.3	3.28	4.0		Blue ice sample
A/CP_A6	1.89	35.1	21.5	34.7	11.3	5.5	1	1.00	4	1	4	5.5	34.4	1.2	0.97	3.8	3.28	5.7		Blue ice sample
A/CP_A7	1.05	78.0	13.6	77.7	13.0	6.3	1	1.00	4	1	4	2.0	77.6	1.2	0.64	4.8	3.28	3.3		Blue ice sample
A/CP_A8	2.18	27.1	27.0	26.3	12.4	6.4	1	1.00	4	1	4	7.3	26.0	1.2	1.11	4.9	3.28	6.0		Blue ice sample
<i>Neumayer</i>																				
A/NM_MB2_3	0.61	117.0	10.0	116.9	16.3	5.7	1	1.00	4	1	4	1.8	116.8	1.2	0.98	4.0	3.28	4.0		Surface sample
A/NM_MB4_6	0.90	93.5	10.4	93.3	11.5	6.1	1	1.00	4	1	4	1.9	93.2	1.2	0.70	4.6	3.28	4.1		Surface sample
A/NM_MB7_8	1.75	39.4	19.6	38.9	11.2	6.4	1	1.00	4	1	4	5.7	38.7	1.2	1.09	5.1	3.28	6.5		Surface sample
A/NM_MB9_11	0.64	98.8	6.9	98.6	10.8	6.0	1	1.00	4	1	4	2.0	98.6	1.2	1.05	4.5	3.28	6.5		Surface sample
<i>Kohnen</i>																				
Surface firn	1.70	13.9	51.5	12.8	30.2	5.3		13.77	4.8	5	4	30.2	11.9	0.4	16.27	3.4	0.84	180.0		Surface sample
<i>Kohnen Drill chip samples</i>																				
DML20_22	2.81	34.6	63.0	34.1	22.4	5.9		2.93	1.0	1	4	8.5	34.1	0.4	2.96	4.4	0.84	8.8	2554.9	3.3
DML24	1.61	27.0	29.1	26.4	18.1	5.7		1.45	2.5	1	4	7.6	26.3	0.4	2.28	4.0	0.84	8.4	2559.6	1.8
DML46_47	2.41	13.0	107.5	11.2	44.7	6.5		3.72	1.3	2	4	10.5	11.2	1.1	2.70	5.1	2.66	8.1	2580.7	2.0
DML48_49	2.91	19.5	87.7	18.4	30.1	6.5		5.42	0.8	2	4	8.7	18.4	1.1	2.70	5.1	2.66	12.0	2582.7	2.2
DML50	3.44	14.1	121.9	12.7	35.5	6.3		4.41	1.3	1	4	8.8	12.6	1.1	3.76	4.8	2.66	7.1	2584.9	1.9
DML51	4.35	15.1	143.3	13.6	33.0	6.5		4.86	2.9	1	4	6.9	13.3	1.1	2.56	5.2	2.66	5.2	2586.8	0.9
DML52	4.10	17.8	149.4	16.6	36.4	6.3		3.99	2.3	1	4	7.2	16.4	1.1	2.34	4.9	2.66	4.3	2590.0	0.9
DML53	3.69	15.1	71.7	14.3	19.4	4.9		2.23	1.5	1	4	11.9	14.2	0.4	2.40	2.9	0.84	8.3	2590.9	1.3
DML54	3.67	14.1	57.2	12.6	15.6	6.3		1.15	1.9	1	4	17.7	12.4	0.4	1.84	4.9	0.84	7.9	2592.2	1.1
DML136+7+8	2.24	17.0	60.1	16.4	26.8	4.5		3.14	1.1	2	4	13.9	16.3	0.4	3.25	2.2	0.84	16.2	2685.2	3.5
DML194_197	1.06	50.3	28.1	50.1	26.4	5.3		5.26	2.3	2	4	4.8	50.0	0.4	3.95	3.5	0.84	20.0	2746.0	2.1
DML211_213	1.38	12.3	321.5	11.2	232.7	5.1		4.38	1.3	2	4	49.3	11.2	0.4	26.08	3.2	0.84	15.0	2759.4	1.0

* The uncertainty of the stratospheric ²⁶Al and ¹⁰Be concentration values is dominated by the uncertainty of the air volume measurement. This cancels out for ²⁶Al/¹⁰Be uncertainty measurements.

References

- Auer, M., Kutschera, W., Priller, A., Wagenbach, D., Wallner, A., Wild, E.M., 2007. Measurement of ^{26}Al for atmospheric and climate research and the potential of $^{26}\text{Al}/^{10}\text{Be}$ ratios. *Nucl. Instr. Meth. B* 259, 595–599.
- Bender, M.L., Barnett, B., Dreyfus, G., Jouzel, J., Porcelli, D., 2008. The contemporary degassing rate of ^{40}Ar from the solid Earth. *Proc. Nat. Acad. Sci.* 105, 8232–8237.
- Burbank, D.W., Leland, J., Fielding, E., Anderson, R.S., Brozovic, N., Reid, M.R., Duncan, C., 1996. Bedrock incision, rock uplift and threshold hillslopes in the northwestern Himalayas. *Nature* 379, 505–510.
- Dash, J.G., Rempel, A.W., Wettlaufer, J.S., 2006. The physics of premelted ice and its geophysical consequences. *Rev. Mod. Phys.* 78, 695–742.
- Delmas, R.J., Beer, J., Synal, H.-A., Muscheler, R., Petit, J.-R., Pourchet, M., 2004. Bomb-test ^{36}Cl measurements in Vostok snow (Antarctica) and the use of ^{36}Cl as a dating tool for deep ice cores. *Tellus* 56 B, 492–498.
- Endt, P.M., 1990. Energy levels of $A=21$ –44 nuclei (VII). *Nucl. Phys. A* 521, 1–830.
- EPICA community members, 2004. Eight glacial cycles from an Antarctic ice core. *Nature* 429, 623–628.
- EPICA community members, 2006. One-to-one coupling of glacial climate variability in Greenland and Antarctica. *Nature* 444, 195–198 and supplementary information.
- Farley, K.A., Patterson, D.B., 1995. A 100-kyr periodicity in the flux of extraterrestrial ^3He to the sea floor. *Nature* 378, 600–603.
- Fink, D., Smith, A., 2007. An inter-comparison of ^{10}Be and ^{26}Al AMS reference standards and the ^{10}Be half-life. *Nucl. Instr. Meth. B* 259, 600–609.
- Honda, M., Imamura, M., 1971. Half-life of ^{53}Mn . *Phys. Rev. C* 4, 1182–1188.
- Horiuchi, K., Matsuzaki, H., Ohta, A., Shibata, Y., Motoyama, H., 2007. Measurement of ^{26}Al in Antarctic ice with the MALT-AMS system at the University of Tokyo. *Nucl. Instr. Meth. B* 259, 625–628.
- Jordan, C.E., Dibb, J.E., Finkel, R.C., 2003. $^{10}\text{Be}/^7\text{Be}$ tracer of atmospheric transport and stratosphere-troposphere exchange. *J. Geophys. Res.* 108, 2–14.
- Kaufmann, P., 2008. Neuentwicklung des Continuous Flow Analysis (CFA) Systems & Messung und Interpretation von EPICA Eisbohrkernen“, PhD thesis, University of Bern.
- Knie, K., Faestermann, T., Korschinek, G., Rugel, G., Rühm, W., Wallner, C., 2000. High-sensitivity AMS for heavy nuclides at the Munich Tandem accelerator. *Nucl. Instr. Meth. B* 172, 717–720.
- Korschinek, G., Bergmaier, A., Faestermann, T., Gerstmann, U.C., Knie, K., Rugel, G., Wallner, A., Dillmann, I., Dollinger, G., Lierse von Gostomski, Ch., Kossert, K., Maiti, M., Poutivtsev, M., Remmert, A., submitted for publication. A new value for the half-life of ^{10}Be by heavy ion elastic recoil detection and liquid scintillation counting, submitted to NIM B.
- Kubo, F.R., 2001. Kosmogene Produktion von Radionukliden, PhD Thesis, Technical University Munich.
- Lal, D., Jull, A.J.T., 2003. Extra-terrestrial influx rates of cosmogenic isotopes and platinum group elements: realizable geochemical effects. *Geochim. Cosmochim. Acta* 67, 4925–4933.
- Lal, D., Peters, B., 1967. Cosmic ray produced radioactivity on the Earth. In: Flüggé, S. (Ed.), *Handbuch der Physik* Bd. 46/2. Springer, Berlin, pp. 551–612.
- Lal, D., Nishiizumi, K., Arnold, J.R., 1987. In situ cosmogenic ^3H , ^{14}C , and ^{10}Be for determining the net accumulation and ablation rates of ice sheets. *J. Geophys. Res.* 92 (B6), 4947–4952.
- Leya, I., Lange, H., Neumann, S., Wieler, R., Michel, R., 2000. The production of cosmogenic nuclides in stony meteoroids by galactic cosmic ray particles. *Meteoritics Planet. Sci.* 35, 258–286.
- Love, S.G., Brownlee, D.E., 1991. Heating and thermal transformation of micrometeoroids entering the Earth's atmosphere. *Icarus* 89, 26–43.
- Luo, S., Ku, T.-L., Wang, L., Southon, J.R., Lund, S.P., Schwartz, M., 2001. ^{26}Al , ^{10}Be and U-Th isotopes in Blake Outer Ridge sediments: implications for past changes in boundary scavenging. *Earth Planet. Sci. Lett.* 185, 135–147.
- Masarik, J., Beer, J., 1999. Simulation of particle fluxes and cosmogenic nuclide production in the Earth's atmosphere. *J. Geophys. Res.* D104 (10), 12099–13012.
- Michel, R., 1999. Long-lived radionuclides as tracers in terrestrial and extraterrestrial matter. *Radiochim. Acta* 87, 47–73.
- Michel, R., Brinkmann, G., Stück, R., 1982. Solar cosmic-ray-produced radionuclides in meteorites. *Earth Planet. Sci. Lett.* 59, 33–48.
- Michel, R., Leya, K., Borges, L., 1996. Production of cosmogenic nuclides in meteoroids: accelerator experiments and model calculations to decipher the cosmic ray record in extraterrestrial matter. *Nucl. Instr. Meth. B* 113, 434–444.
- Michelmayer, L., 2007. Isobar separation with post-stripping for the measurement of cosmogenic ^{10}Be at VERA. Diploma Thesis, Isotope Research Group, Faculty of Physics, University Vienna.
- Middleton, R., Klein, J., 1987. ^{26}Al : measurements and applications. *Phil. Transact. Royal Society London* A323, 121.
- Middleton, R., Klein, J., Raisbeck, G.M., Yiou, F., 1983. Accelerator mass spectrometry with ^{26}Al . *Nucl. Instr. Meth.* 218, 430–438.
- Nakamura, T., Sugita, H., Imamura, M., Uwamino, Y., Shibata, J.S., Nagai, H., Takehatake, M., Kobayashi, K., 1992. Measurement of long-lived ^{10}Be , ^{14}C and ^{26}Al production cross sections for 10–40 MeV neutrons by accelerator mass spectrometry. In: Quaim, S.M. (Ed.), *Nuclear Data for Science and Technology*. Springer, New York, pp. 714–716.
- Nishiizumi, K., Klein, J., Middleton, R., Elmore, D., Kubik, P.W., Arnold, J.R., 1986. Exposure history of Shergottites. *Geochim. Cosmochim. Acta* 50, 1017–1021.
- Nishiizumi, K., Kohl, C.P., Shoemaker, E.M., Arnold, J.R., Klein, J., Fink, D., Middleton, R., 1991. *In situ* ^{10}Be – ^{26}Al exposure ages at Meteor Crater, Arizona. *Geochim. Cosmochim. Acta* 55, 2699–2703.
- Nishiizumi, K., Arnold, J.R., Brownlee, D.E., Caffee, M.W., Finkel, R.C., Harvey, R.P., 1995. Beryllium-10 and Aluminum-26 in individual cosmic spherules from Antarctica. *Meteoritics* 30, 728–732.
- Nishiizumi, K., Imamura, M., Caffee, M.W., Southon, J.R., Finkel, R.C., McAninch, J., 2007. Absolute calibration of ^{10}Be AMS standards. *Nucl. Instr. Meth. B* 258, 403–413.
- Norris, T.L., Gancarz, A.J., Rokop D.J., Thomas, K.W., 1983. Half-Life of ^{26}Al . *J. Geophys. Res.* 88 (S1), B331–B333.
- Pavicevic, M.K., Wild, E.M., Priller, A., Kutschera, W., Boev, B., Prohaska, T., Berger, M., Steffan, I., 2004. AMS measurements of ^{26}Al in quartz to assess the cosmic ray background for the geochemical solar neutrino LOREX. *Nucl. Instr. Meth. B* 223–224, 660–667.
- Priller, A., Berger, M., Gäggeler, H., Gerasopoulos, E., Kubik, P.W., Schnabel, C., Tobler, L., Wild, E.M., Zanis, P., Zerefos, C., 2004. Accelerator mass spectrometry of particle-bound ^{10}Be . *Nucl. Instr. Meth. B* 223–224, 601–607.
- Raisbeck, G.M., Yiou, F., Klein, J., Middleton, R., 1983. Accelerator mass spectrometry measurement of cosmogenic ^{26}Al in terrestrial and extraterrestrial matter. *Nature* 301, 690–692.
- Raisbeck, G.M., Yiou, F., Cattani, O., Jouzel, J., 2006. ^{10}Be evidence for the Matuyama–Brunhes geomagnetic reversal in the EPICA Dome C ice core. *Nature* 444, 82–84.
- Reedy, R.C., 1990. Cosmogenic-radionuclide production rates in mini-spherules. *Lunar Planet. Sci.* 21, 1001–1002.
- Rempel, A.W., Wettlaufer, J.S., 2003. Segregation, transport and interaction of climate proxies in polychrystalline ice. *Can. J. Phys.* 81, 89–97.
- Reyss, J.-L., Yokoyama, Y., Guichard, F., 1981. Production cross sections of ^{26}Al , ^{22}Na , ^7Be from argon and of ^{10}Be , ^7Be from nitrogen: implications for production rates of ^{26}Al and ^{10}Be in the atmosphere. *Earth Planet. Sci. Lett.* 53, 203–210.
- Röthlisberger, R., Mulvaney, R., Wolff, E.W., Hutterli, M.A., Bigler, M., de Angelis, M., Hansson, M.E., Steffensen, J.P., Udisti, R., 2003. Limited dechlorination of sea-salt aerosols during the last glacial period: evidence from the European Project for Ice Coring in Antarctica (EPICA) Dome C ice core. *J. Geophys. Res. Atmos.* 108 (16), 4526. doi:10.1029/2003JD003604.
- Ruth, U., Barnola, J.-M., Beer, J., Bigler, M., Blunier, T., Castellano, E., Fischer, H., Fundel, F., Huybrechts, P., Kaufmann, P., Kipfstuhl, S., Lambrecht, A., Morganti, A., Oerter, H., Parrenin, F., Rybak, O., Severi, M., Udisti, R., Wilhelms, F., Wolff, E., 2007. “EDML1”: A chronology for the EPICA deep ice core from Dronning Maud Land, Antarctica, over the last 150000 years. *Clim. Past* 3, 475–484.
- Samworth, E.A., Warburton, E.K., Engelbertink, G.A.P., 1972. Beta decay of the ^{26}Al ground state. *Phys. Rev. C* 5, 138–142.
- Schäfer, J.M., Baur, H., Denton, G.H., Ivy-Ochs, S., Marchant, D.R., Schlüchter, C., Wieler, R., 2000. The oldest ice on Earth in Beacon Valley, Antarctica: new evidence from surface exposure dating. *Earth Planet. Sci. Lett.* 179, 91–99.
- Schlosser, E., Lipzig, N., Oerter, H., 2002. Temporal variability of accumulation at Neumayer station, Antarctica, from stake array measurements and a regional atmospheric model. *J. Glac.* 48, 87–94.
- Strack, E., Heisinger, B., Dockhorn, B., Hartmann, F.J., Korschinek, G., Nolte, E., 1994. Determination of erosion rates with cosmogenic ^{26}Al . *Nucl. Instr. Meth. B* 92, 317–320.
- Sugden, D.E., Marchant, D.R., Potter, N., Souchez Jr., R.A., Denton, G.H., Swisher III, C.C., Tison, J.-L., 1995. Preservation of Miocene glacier ice in East Antarctica. *Nature* 376, 412–414.
- Tanaka, S., Sakamoto, K., Komura, K., 1972. Aluminium 26 and Manganese 53 produced by Solar-Flare particles in lunar rock and cosmic dust. *J. Geophys. Res.* 77, 4281–4288.
- Thomas, J.H., Rau, R.L., Skelton, R.T., Kavanagh, R.W., 1984. Half-life of ^{26}Al . *Phys. Rev. C* 30, 385–387.
- Wagenbach, D., 1994. Coastal Antarctica: atmospheric chemical composition and atmospheric transport. In: Wolff, E., Bates, R. (Eds.), *Chemical Exchange between the Atmosphere and Polar Snow NATO ARW Workshop II Chiocci, Italy, 1995*. NATO ASI Series I, vol. 43. Springer, Berlin, pp. 173–199.
- Wagenbach, D., Legrand, M., Fischer, H., Pichlmayer, F., Wolff, E.W., 1998. Atmospheric near-surface nitrate at coastal Antarctic sites. *J. Geophys. Res.* 103, 11007–11020.
- Wallner, A., Ikeda, Y., Kutschera, W., Priller, A., Steier, P., Vonach, H., Wild, E.M., 2000. Precision and accuracy of ^{26}Al measurements at VERA. *Nucl. Instr. Meth. B* 172, 382.
- Wang, L., Ku, T.L., Luo, S., Southon, J.R., Kusakabe, M., 1996. ^{26}Al – ^{10}Be systematics in deep sea sediments. *Geochim. Cosmochim. Acta* 60, 109–119.
- Weller, R., Trauffetter, F., Fischer, H., Oerter, H., Piel, C., Miller, H., 2004. Post depositional losses of methane sulfonate, nitrate, and chloride at the EPICA deep-drilling site in Dronning Maud Land, Antarctica. *J. Geophys. Res.* 109, D07301. doi:10.1029/2003JD004189.
- Willerslev, E., et al., 2007. Ancient biomolecules from deep ice cores reveal a forested southern Greenland. *Science* 317, 111–114.
- Winkler, G., Fischer, H., 2006. 30,000 years of cosmic dust in Antarctic ice. *Science* 313, 491.